APEM journal
Advances in Production Engineering & Management 6 (2011) 2, 105-116
ISSN 1854-6250 Scientific paper

UPSET-FORGING OF SINTERED ALUMINIUM TRUNCATED CONICAL PREFORMS

Mohanty, T.* & Singh, S.*
*School of Mechanical Engineering
KIIT University, Patia, Bhubaneswar-751024
E-mail ssingh@kiit.ac.in; saranjitkiit@gmail.com

Abstract:
The present paper deals with both theoretical and experimental investigations of upset-forging of sintered aluminium truncated conical preforms. The analysis considers heterogeneous deformation of preform slant sides, composite die-workpiece interfacial friction, preform densification and inertia effects. The expressions for exponential velocity field, strain rates, average forging load and preform bulged profile were established based on the Upper Bound approach. The experiments were conducted on sintered preforms prepared by compacting aluminium metal powder in closed dies. The effect of interfacial friction, die speed, preform shape and die speed on the bulged profile, strain rates, relative density, inertia energy dissipation and average die load was studied. Also, the interaction between die load, die velocity and formability was investigated using DOE (Design of Experiments) and RSM (Response Surface Methodology) techniques. The experimental and theoretical results were found in good agreement and it is expected that the present work will be useful for the assessment of deformation characteristics during processing of sintered materials.

Key Words: Upset-Forging, Truncated Conical Preform, Die Velocity, Forging Load

Nomenclature

a_{ij}	acceleration field	U_{ij}	velocity field
$\dot{\varepsilon}_{ij}$	strain rate field	U	die velocity
ΔU	interfacial relative velocity	$\dot{U}$	die acceleration
p	die pressure	F_{av}	average forging load
S	surface area	V	volume
r_i	small radius of conical preform	r_o	large radius of conical preform
r_m	sticking zone radius	r'	radius of elemental strip
$\delta r'$	radial bulge of elemental strip	H_0	initial height of conical preform
t_c	compression time	dz	distance moved by die time 't_c'
W_i	internal energy dissipation	W_f	friction energy dissipation
W_a	inertia energy dissipation	J	external energy supplied
σ_o	flow stress of preform	τ	frictional shear stress
σ_m	hydrostatic stress	J_2	second invariant of stress
n	constant quantity	β	barreling factor
η	constant function of ρ_0	α	half cone angle of preform
ρ_0	preform relative density	C_f	shape-complexity factor
μ	coefficient of friction	ϕ_o	specific cohesion factor
ξ	inertia factor	ζ	load factor

Subscripts

r	radial
z	axial
θ	circumferential

1. INTRODUCTION

Upset-forging of sintered materials, i.e. sinter-forging is a net-shape manufacturing technology for the mass production of high performance and precise engineering components at competitive rates, virtually without scrap losses, whose mechanical and metallurgical properties compares favorably with the corresponding wrought products [1,2]. The technology uses sintered preforms as starting material manufactured by powder metallurgy route. Thus, it combines the advantages associated with powder metallurgy and conventional forging processes. Powder metallurgy provides the sound metallurgical structure as well as, avoids large number of energy intensive operations and subsequent forging provides adequate mechanical properties to the final sinter-forged products by eliminating porosity. The technology has extensive applications in almost all the major industries with large number of precise components, e.g. connecting rods, gears, crankshafts, engine valves etc [3, 4]. The analysis during forging of sintered materials have been reported by different researchers from various aspects using simple generic shapes [5-13], but no attempt has been made so far to investigate the upsetting of sintered axi-symmetric truncated conical preforms.

The sinter-forging process is entirely different from the conventional-forging of wrought metal, as characteristic of porous materials during compression has to be considered. During sinter-forging, volumetric constancy is no longer valid for establishing the compatibility conditions, as relative density of the compacts increase simultaneously with the deformation due to closing of inter-particle pores. Thus, yielding of sintered powder preforms is sensitive to hydrostatic stresses. The deformation pattern is influenced by several factors interacting with each other in the complex manner, e.g. perform relative density, die-workpiece interfacial friction conditions, flow stress of sintered material, die speed and contact time under load. The prediction of these factors, their interaction and influence on various deformation characteristics are very important to completely understand the mechanics involved during sinter-forging process and to obtain a realistic measure of average die load involved during deformation. The present paper aims at analyzing various deformation characteristics during upsetting of truncated conical preform considering heterogeneous deformation due to barreling of slant sides, composite die-workpiece interfacial friction conditions, densification of preform along with compression and inertia effects. The experiments were conducted by upsetting sintered truncated conical preforms in a mechatronic press. The effect of die speed i.e. dynamic effects on average die load has been critically studied using inertia and load factors.

2. UPSET-FORGING CHARACTERISTICS

The deformation of a sintered preforms during cold upset-forging is influenced by several important factors like die-workpiece interfacial friction conditions, densification, barreling and yield criterion. These characteristics need to be suitably formulated to emulate the real deformation process, so that theoretical results are in agreement with experimental ones.

2.1 Die-Workpiece Interfacial Friction [28-30]

During upset-forging process, die-workpiece interfacial lubrication film is broken and conditions essential for adhesion friction are created. The flow pattern of sintered materials suggests presence of two interfacial friction zones *i.e.* an inner zone with no relative movement between die and workpiece surface (sticking zone) and an outer sliding zone. Thus, interfacial frictional condition is composite in nature and includes both sliding and sticking frictions and the corresponding shear stress is given as follows:

$$|\tau|_h = \mu\left\{p + \rho_0\phi_0\left[1 - \left(\frac{r_m - r}{n|r|_h}\right)\right]\right\} \tag{1}$$

where: $$r_m = r_o - \frac{H_0}{2\mu}\ln\left(\frac{1}{\mu\sqrt{3}}\right) \quad (2)$$

2.2 Densification [31, 32]

During investigation of plastic deformation of powder preforms, it was revealed that compressive forces gradually close down the pores leading to decrease in volume and subsequently increase in relative density of preforms, which almost approaches apparent density at the end of process. This is attributed due to asymptotic increase in real die-workpiece contact area. Thus, yielding of sintered materials is sensitive to compressive hydrostatic stress component and an appropriate yield criterion and compatibility condition for porous materials has to be considered, which are given as follows:

$$\rho^k\sigma_0 = \sqrt{3}J_2 \pm 3\eta\sigma_m \quad (3)$$

$$\dot{\varepsilon}_r + \left[\frac{(1-2\eta)}{2(1+\eta)}\right]\dot{\varepsilon}_z = 0 \quad (4)$$

where, $$\eta = 0.54(1-\rho_0)^{1.2} \quad (5)$$

2.3. Barreling

The conical free surface of preform bulge out during upset-forging and its magnitude mainly depends on initial relative density of preform and degree of frictional constraint at die-workpiece interface. In case of lubricated preforms *i.e.* low friction conditions, the radial flow of preform is homogeneous and uniform throughout the surface and hence barreling is less. But, in case of unlubricated preforms *i.e.* high friction conditions, the radial flow at the center of preform height is considerably more as compared to die-workpiece interface surfaces and hence bulge is more (refer Figure 1). The bulging of preform is considered in the present analysis by introducing a barreling factor ‘β’.

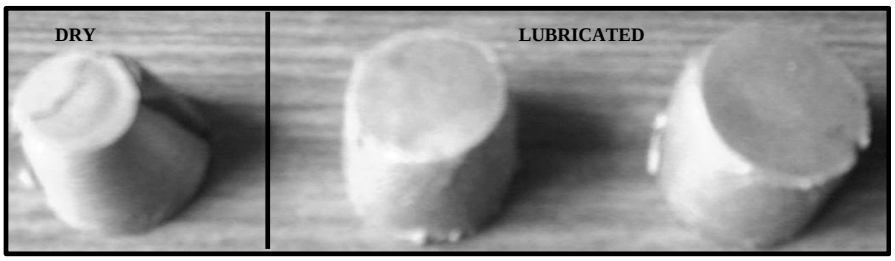

Figure 1: Upset-Forged Truncated Conical Sintered Preforms under Dry and Lubricated Interfacial Friction Conditions.

3. THEORETICAL ANALYSIS

The following assumptions are made in the present analysis:

- The friction due to adhesion is a function of relative density.
- The compression of sintered materials takes place along with compaction.
- The yielding of sintered materials is sensitive to hydrostatic stress.
- The compatibility equation is derived from volume inconstancy principle.
- The bulging of truncated conical preform is concentrated at the lower radius.

3.1. Average Die Load

The upset-forging of truncated conical sintered preform is considered in-between two perfectly flat, parallel and rigid die platens, where upper die platen is stationary and lower die platen is moving upwards with velocity 'U'. The boundary conditions are as follows:

$$U_r = U \quad \text{at} \quad z = 0 \tag{6}$$

$$U_r = 0 \quad \text{at} \quad z = H_0 \tag{7}$$

Velocity field and corresponding strain rates taking bulging into consideration and satisfying the equations (4), (6) and (7) are given as follows:

$$U_r = \left[\frac{(1-2\eta)\beta e^{-\beta z/H_0} Ur}{2(1+\eta)(1-e^{-\beta})H_0} \right] \tag{8}$$

$$U_z = -\left[\frac{\left(e^{-\beta} - e^{-\beta z/H_0}\right)U}{\left(1-e^{-\beta}\right)} \right] \tag{9}$$

$$U_\theta = 0 \tag{10}$$

$$\dot{\varepsilon}_{rr} = \frac{\partial U_r}{\partial r} = \left[\frac{(1-2\eta)\beta e^{-\beta z/H_0} U}{2(1+\eta)(1-e^{-\beta})H_0} \right] \tag{11}$$

$$\dot{\varepsilon}_{zz} = \frac{\partial U_z}{\partial z} = -\left[\frac{\beta e^{-\beta z/H_0} U}{H_0\left(1-e^{-\beta}\right)} \right] \tag{12}$$

$$\dot{\varepsilon}_{\theta\theta} = \frac{U_r}{r} = \left[\frac{(1-2\eta)\beta e^{-\beta z/H_0} U}{2(1+\eta)(1-e^{-\beta})H_0} \right] \tag{13}$$

$$\dot{\varepsilon}_{rz} = \frac{1}{2}\left(\frac{\partial U_r}{\partial z} + \frac{\partial U_z}{\partial r} \right) = -\left[\frac{(1-2\eta)\beta^2 e^{-\beta z/H_0} Ur}{4(1+\eta)(1-e^{-\beta})H_0^2} \right] \tag{14}$$

$$\dot{\varepsilon}_{r\theta} = \dot{\varepsilon}_{\theta z} = 0 \tag{15}$$

The external energy 'J' supplied by die platens during plastic deformation based on *Upper Bound* approach [33] is given as follows:

$$J = \frac{2\sigma_o}{\sqrt{3}} \int_V \sqrt{\frac{1}{2}\dot{\varepsilon}_{ij}\dot{\varepsilon}_{ij}}\, dV + \int_S \tau |\Delta U| dS + \int_V \rho_p (a_i U_i) dV \tag{16}$$

The first term denotes rate of internal energy dissipation 'W_i', second term denotes frictional shear energy dissipation 'W_f' and last term denotes energy dissipation due to inertia forces 'W_a'. Substituting equations (8) to (15) into above equation and solving separately, the internal, frictional and inertia energy of dissipations are given as follows:

$$W_i = \left(\frac{2\sigma_o}{\sqrt{3}}\right)\int_{z=0}^{z=H_0}\int_{r=r_i}^{r=(r_i+H_0\tan\alpha)}\left[\sqrt{\dot{\varepsilon}^2{}_{rr} + \frac{1}{2}\left(\dot{\varepsilon}^2{}_{zz} + \dot{\varepsilon}^2{}_{rz}\right)}\right](2\pi r dr dz)$$
$$= \left[\frac{8\pi\sigma_o U(\psi-2)^{1/2}H_0^2}{3\sqrt{3}\beta^2}\right]\left[\psi + \frac{\beta^2 r_i^2\left(1-\tan^2\alpha\right)}{4H_0^2}\right]^{3/2} \tag{17}$$

$$W_f = [\ ]\int_{r=0}^{r=r_0}\left[|\tau|_{z=H_0}|U_r|_{z=H_0}\right](2\pi r)dr + \int_{r=0}^{r=r_i}\left[|\tau|_{z=0}|U_r|_{z=0}\right](2\pi r)dr$$
$$= \left[\frac{\pi\mu(1-2\eta)\beta U r_i^2}{6(1+\eta)\left(1-e^{-\beta H_0}\right)}\right]\left\{\begin{array}{l}\left[\left[Pav + r_i^3\rho_0\phi_0\left(1+\frac{3}{4n}\right)\right]\left(\frac{r_0^3}{r_i^3}e^{-\beta H_0}+1\right)\right] \\ -\left(\frac{r_m}{nr_i^3}\right)\left(r_0^2 e^{-\beta H_0} + r_i^2\right)\end{array}\right\} \tag{18}$$

$$W_a = \int_{z=0}^{z=H_0}\int_{r=0}^{r=(r_i+H_0\tan\alpha)}\left\{\left[\rho_i\left(a_r U_r + a_z U_z\right)\right](2\pi r)drdz\right\}$$
$$= \left(\pi\rho_i r_i^2\right)\left(\frac{r_i}{H_0}+\tan\alpha\right)^2\left\{\left\{\left[\frac{(1-2\eta)^2\left(r_i/H_0+\tan\alpha\right)^2 U^3\left(1+e^{-\beta H_0}\right)}{64(1+\eta)^2}\right]\right\} + \frac{U^3}{3} + U\dot{U}H_0\right\} \tag{19}$$
$$\times\left[1-\frac{3(1-2\eta)\left(1+e^{-2\beta H_0}\right)}{8(1+\eta)}\right]$$

where, $\psi = \left\{2+\left[\frac{2(1+\eta)}{1-2\eta}\right]^2\right\}$

Average forging load can be computed by substituting equations (17) to (19) into following equation:

$$F_{av} = J(U)^{-1}A_{av} \tag{20}$$

3.2. Average Bulged Radius

Consider an elemental strip of thickness ‘dh’ and radius ‘r'’ at a distance ‘h’ from lower die platen during upset-forging of truncated conical sintered preform. Assume that elemental strip bulges radially by an amount ‘$\delta r'$’, when lower die has moved through a distance ‘dz’ in time interval ‘t_c’, the final bulged radius of this elemental strip may be given as follows:

$$\left(r'+\delta r'\right) = r'\left[1+\frac{(1-2\eta)\beta e^{-\beta h}dz}{4(1+\eta)\left(1-e^{-\beta H_0}\right)}\right] \tag{21}$$

The shape-complexity factor *‘C_f’* is defined as follows:

$$C_f = \left(\frac{r_0}{r_i}\right) = \left(\frac{r_i + H_0\tan\alpha}{r_i}\right) = \left(1+\frac{H_0\tan\alpha}{r_i}\right) \tag{22}$$

The inertia factor 'ξ' and load factor 'ζ' respectively are defined as follows:

$$\xi(\%) = \left(\frac{W_a}{J}\right)100 \tag{23}$$

$$\zeta(\%) = \left(\left|\frac{|F_{av}|_{withdynamiceffects} - |F_{av}|_{withoutdynamiceffects}}{|F_{av}|_{withdynamiceffects}}\right|\right)100 \tag{24}$$

4. EXPERIMENTAL WORK

Experiments were conducted on the truncated conical preforms prepared by compacting aluminium powder in a graphite lubricated die having bore diameter of 30 mm at pressure of about 15 tonf. Table I shows the physical and chemical properties of aluminium powder used. The green compacts were sintered at about 400^0C for four hours in an endothermic sand atmosphere. The compacts were then wrapped in a Teflon sheet and repressed at same compaction pressure in the same die and re-sintered to same temperature and time to obtain uniform density distribution. These compacts were than machined to the required dimensions and were finally polished with coarse and fine emery papers respectively. The density of preforms was obtained simply by measuring their dimensions and weight and relative density was obtained by taking the ratio of density of preform to that of density of solid metal. The final upsetting experiments were conducted on a 100-ton hydraulic press.

Table I: Physical and Chemical Characteristics of Aluminium Metal Powder.

Particle size (microns)	Weight Under (%)	Chemical Analysis	Weight (%)
118.0	100.0	Aluminium	99.500
88.1	98.9	Iron	< 0.1700
65.6	95.5	Silicon	< 0.1313
48.8	88.8	Zinc	< 0.0053
36.3	79.0	Manganese	< 0.0023
27.0	65.8	Magnesium	< 0.0016
17.4	40.1	Apparent density	1.25 gm / c.c.
13.0	25.5	Tap density	1.50 gm / c.c.

5. DESIGN OF EXPERIMENT (DOE) ANALYSIS [34, 35]

The two level (2^n) full factorial randomized DOE and RSM techniques has been used to study the interrelationship between important deformation characteristics and their influence on dynamic effects during upset-forging of truncated conical preform. The analysis considers four *'Factors'*, *e.g.* shape-complexity factor (A), barrelling parameter (B), initial relative density (C) and die velocity (D) and two *'Response Variable'*, *i.e.* inertia and load factors. The factor levels are shown in table II.

Table III shows the *'Coefficient of Factor Effect Estimate'*, *'Sum of Squares'* and *'Percent Contribution'* for each experiment run for inertia and load factors. It is evident from the table that *'Interaction Effects'* between initial preform relative density and die velocity (CD) are prominent. Further, these interactions are investigated using RSM technique and multiple linear regression equations of second order have been formulated mathematically [Refer Equations 25 and 26] and three-dimensional graphs have been generated using MATLAB software.

$$|Y_{cd}|_{inertiafactor} = 40.09 - 55.28C + 1.82D + 11.92C^2 - 0.29D^2 - 7.08CD + 1.6C^2D^2 \tag{25}$$

$$\left|Y_{cd}\right|_{loadfactor} = 12.83 - 18.85C - 4.69D + 35.97C^2 - 1.16D^2 - 5.94CD + 1.28C^2D^2 \qquad (26)$$

Table II: Factor Levels during DOE Analysis.

Factors	Factor Description		Levels	
			Low	High
A	Shape-complexity factor	(C_f)	1.1	1.6
B	Barrelling parameter	(β)	0.30	0.40
C	Initial relative density	(ρ_0)	0.70	0.90
D	Die Velocity	(U)	0.01 m/s	10 m/s

Table III: Factor Effect Estimate and Percent Contribution for Inertia and Load Factors.

Factor Effect	Factor Effect Estimate for		Sum of Squares for		Percent Contribution for	
	Inertia Factor	Load Factor	Inertia Factor	Load Factor	Inertia Factor	Load Factor
A	7.08E+00	7.18E+00	2.01E+02	2.06E+02	2.35E+01	7.52E+00
B	3.12E-01	2.49E+00	3.90E-01	2.47E+01	4.56E-02	9.02E-01
AB	2.68E-01	-9.36E-02	2.87E-01	3.51E-02	3.36E-02	1.28E-03
C	1.97E+00	4.83E+00	1.55E+01	9.33E+01	1.81E+00	3.40E+00
AC	1.37E+00	5.75E-01	7.50E+00	1.32E+00	8.76E-01	4.83E-02
BC	1.41E-01	-5.47E-01	7.90E-02	1.20E+00	9.23E-03	4.36E-02
ABC	3.43E-02	-6.04E-01	4.69E-03	1.46E+00	5.49E-04	5.32E-02
D	1.02E+01	-2.38E+01	4.20E+02	2.26E+03	4.91E+01	8.24E+01
AD	6.88E+00	-4.84E+00	1.89E+02	9.37E+01	2.21E-01	3.42E-01
BD	3.71E-01	-1.34E+00	5.49E-01	7.14E+00	6.42E-02	2.61E-01
ABD	3.43E-02	-6.04E-01	4.69E-03	1.46E+00	5.49E-04	5.32E-02
CD	1.95E+00	-3.57E+00	1.53E+01	5.10E+01	3.79E+00	4.56E+00
ACD	1.24E+00	-3.35E-01	6.19E+00	4.50E-01	7.24E-01	1.64E-02
BCD	6.40E-02	3.69E-02	1.64E-02	5.44E-03	1.92E-03	1.98E-04
ABCD	1.04E-01	4.56E-01	4.31E-02	8.33E-01	5.03E-03	3.04E-02

6. RESULTS AND DISCUSSION

To illustrate the effect of various deformation characteristics and die speed on inertia energy dissipation, die load and strains rates involved during upset-forging of truncated conical sintered preform, a typical data has been considered as: H_0 = 17 mm, r_0 = 12 mm, β = 0.35, $\rho_0\phi_0 = 0.3P_{av}$, μ = 0.3, n = 2, $\rho_i = 2 \times 10^3$ kg/m^3, σ_0 = 6.25 N/mm^2 and C_f = 1.6, 1.3 and 1.1 ($\alpha = 15^0$, 10^0 and 5^0 respectively).

Figure 2 and Figure 3 shows the variation of inertia energy dissipation and inertia factor respectively with die velocity for different shape-complexity factors. It is clearly evident that inertia energy dissipation and inertia factor increases exponentially with increase in the die velocity. The inertia factor becomes asymptote to y-axis at the end of operation, indicating that inertia energy dissipation is appreciably high at high deformation speed. Also, the curves are higher for low shape-complexity factors indicating that as the shape of conical sintered preform approaches towards that of an enclosing cylinder, inertial energy requirement increases.

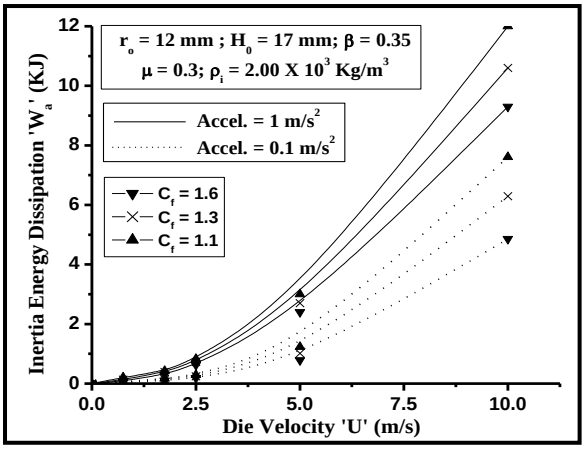

Figure 2: Variation of Inertia Energy Dissipation with Die Velocity.

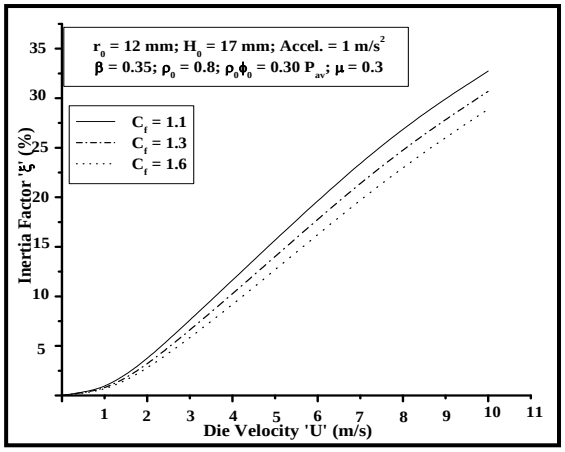

Figure 3: Variation of Inertia Factor Dissipation with Die Velocity.

Figure 4 and Figure 5 shows the variation of average forging load and load factor respectively with die velocity. It is apparent from the fi gures that average die load and load factor decreases exponentially with increase in die velocity. The reason for decrease in die load is attributed to small contact time under die load at high deformation speed, which does not allow the internal heat generated during deformation to dissipate quickly. Also, the die load requirement is higher for lower shape-complexity factor due to higher sintered material associated with them.

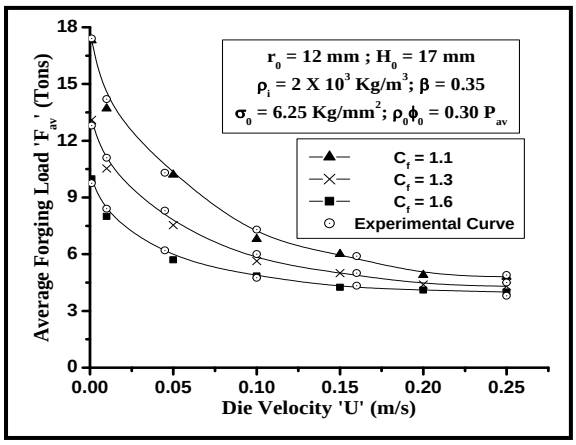

Figure 4: Variation of Average Forging Load with Die Velocity.

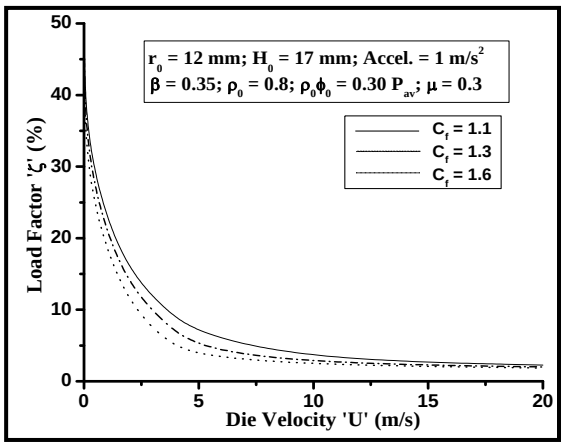

Figure 5: Variation of Load Factor with Die Velocity.

Figure 6 shows the variation of small and large radii of truncated conical preform. It can be seen that percent change in smaller diameter is higher than that of larger diameter for same die velocity. It is due to higher interfacial friction at the larger end of preform. Thus, it is concluded that the deformation during sinter-forging of truncated conical preform is primarily concentrated at its smaller radius. Figure 7 shows the variation of radial and axial strain rate with preform height reduction for different die velocity. It can be seen that both radial and axial strain rates increases exponentially with preform height reduction. Also, the axial strain rate increases, whereas radial strain rate decreases with die velocity. The strain rates encountered during upset-forging at higher speed are considerably high *e.g.* 1500 s^{-1} approx at 40-percentage height reduction for die velocity of 5 m/s.

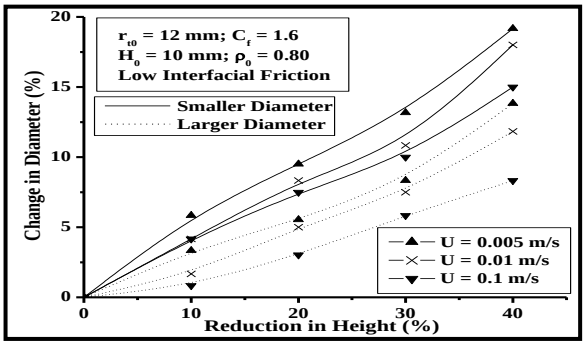

Figure 6: Variation of small and large radii of truncated conical preform.

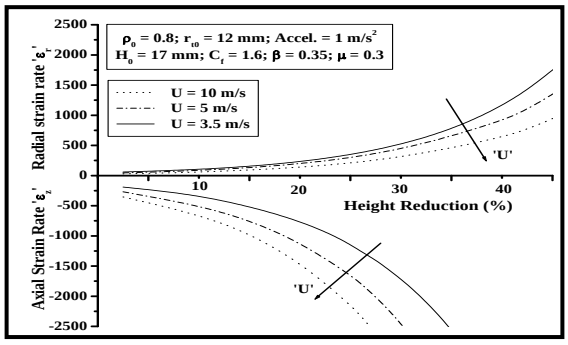

Figure 7: Variation of axial and radial strain rates with die velocity.

The bulging of truncated conical sintered preform is shown in Figure 8 and only half of preform has been considered for analysis due to its symmetry about vertical axis. It is evident that as lower die travel increases preform barrels and its bulge increases. This is due to the formation of conical wedge of relatively undeformed metal immediately below the preform surface, where die-workpiece interfacial friction retards its plastic flow. The rest of preform surface experiences high strains and bulges out in the form of a barrel. It is also seen that bulging of truncated conical sintered preform is concentrated at lower radius because the frictional shear stress is low at smaller end of the truncated conical preform. Figure 9 shows the variation of relative density with percent height reduction for different shape-complexity factors and interfacial friction conditions. It is clear that relative density of truncated conical sintered preform increases with deformation and becomes comparable to that of wrought metals at the end of operation.

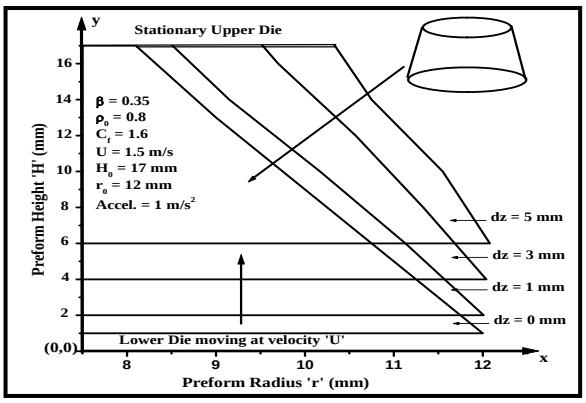

Figure 8: Bulging of truncated conical sintered preform with die travel.

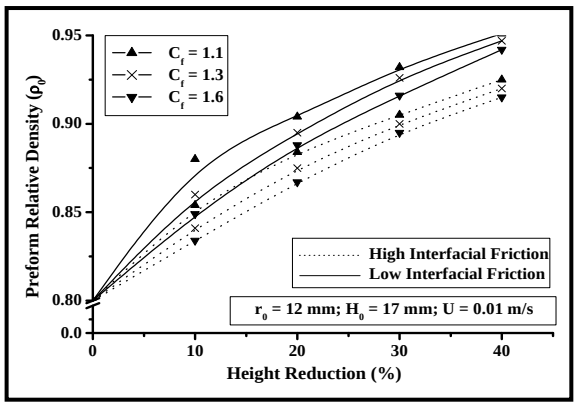

Figure 9: Variation of preform relative density with height reduction.

Figure 10 shows the photomicrograph of pores on top surface of aluminium powder preforms sintered at 400^0 C temperature for four hours at 0, 15, 30 and 40 percent of height reductions respectively. It is clearly apparent from the figures that powder particles consolidate and pores close down with the application of compressive load during progress of the forging process. Also, the densification of preform takes place simultaneously with the deformation. Figure 11 shows the variation of load ratio with height reduction of preform, up to 42 percent of height reduction, which is the maximum formability of sintered materials observed during present study. It is clearly evident that load ratio increases with height reduction and reaches to unity at about 20 percent height reduction. The values of load ratio higher than unity indicates that die load required to carry the forging operation at U = 0.25 m/s is smaller than that at U = 0.001 m/s for all other deformations conditions remaining same, which indicates that die loads are higher for higher die velocity till 20 percent of height reduction. Thereafter, there is drastic decrease in the die load with increase in the die velocity. This is due to the predominance of strain rate effect and reduced chilling during height reduction more than 20 percent. The rate of decrease in die load also slightly decreases about maximum preform

formability, due to the onset of fracture. The above two die velocities were selected merely on the basis of availability of die speeds on the mechatronic press.

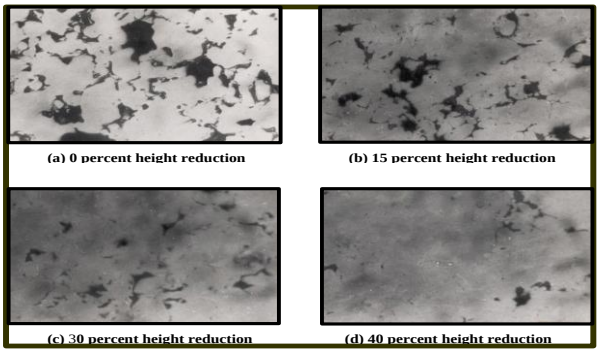

Figure 10: Photomicrographs of pores on preform surface for different height reductions.

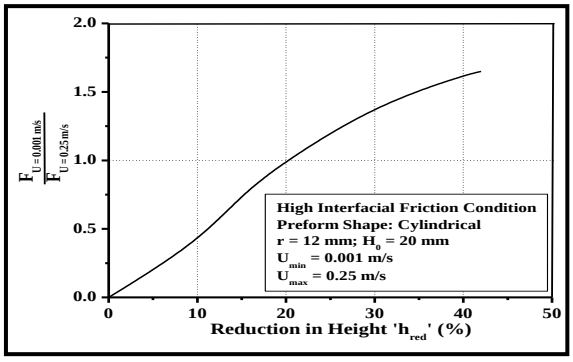

Figure 11: Variation of load ratio with percent height reduction.

Figure 12 (a) and (b) shows the interaction effects *'C-D'* for inertia and load factors respectively in form of 3-D response surfaces. It is clearly evident that inertia factor increases linearly with the increase in both die velocity and preform relative density. This shows that magnitude of inertia energy dissipation becomes comparable with those of internal and frictional shear energy dissipations, especially at higher die velocities. Hence, it must be considered during the analysis for accurate prediction of die loads. It is also apparent that load factor decreases exponentially with increase in die velocity, whereas increases slightly with increase in preform relative density. This suggests that die velocity is the most critical deformation characteristics during mechanical processing of sintered materials, whose effects on the inertia energy dissipation and average die load becomes pronounced at higher deformation speeds.

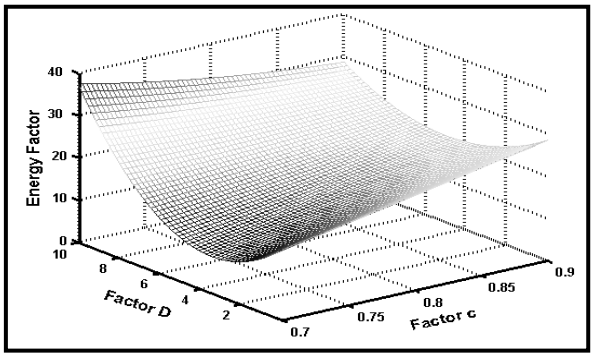

Figure 12 (a): Interaction effect *'C-D'* with inertia factor.

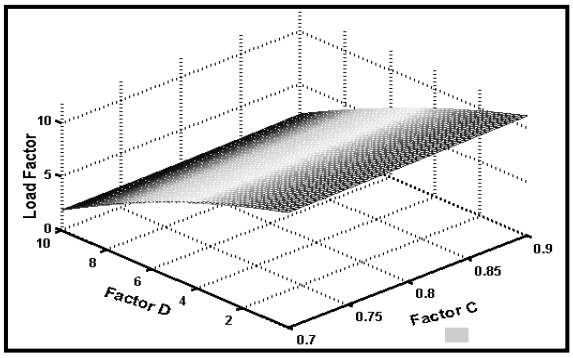

Figure 12 (b): Interaction effect *'C-D'* with load factor.

7. CONCLUSIONS

The major conclusions from the present research work may be summarized as follows:

- The relative density of truncated conical preform increases with increase in die velocity, forging load and preform height reduction and becomes comparable with wrought materials at the end of forging operation. The present upset-forging is characterized by high magnitude of strain rates in the order of 2000 s^{-1} approx.
- The inertia energy dissipation has been found to increase with die velocity and become comparable with other energy dissipations at higher deformation speeds. The dynamic effects on relative magnitudes of various energy dissipations has been illustrated using inertia factor *'ξ'*, which has been found to increase exponentially with die velocity.
- The forging load and load factor *'ζ'* has been found to decrease with die velocity and is appreciably low at higher die speeds. This is because higher die speeds lead to

very small contact time under load and restricts the internal heat generated during upset-forging to dissipate quickly reducing the resistance of sintered materials against deformation. Also, the energy and load requirements are higher for enclosing shapes of preform.

- There has been a complex interaction among maximum height reduction, die velocity and die load during upset-forging of truncated conical preform, which was demonstrated using load ratio, which has been found to increases with height reduction and attains unity value for about 20 percent height reduction. This signifies that die load decrease considerably with the increase in die velocity for height reductions higher than 20 percent due to the predominance of strain rate effect. The reductions in the die load become significant only after 20 percent of height reduction, which may vary with the two limits of die velocities considered during present investigation.
- The DOE and RSM techniques were employed successfully for the analysis of various deformation characteristics during upset-forging of truncated conical preform. It was found that both the interaction effects between die velocity and preform relative density are of significant importance. The multiple linear regression equations of second order and the corresponding three-dimensional graphs were used to depict these interaction effects. It was found that increase in the die velocity results into increase in the inertia factor and decrease in the load factor appreciably, *e.g.* increase in die velocity increases the inertia energy dissipation, as a fraction of total external energy supplied by the die platens and decreases the die load requirements.
- It is expected that the present research work will be highly useful for understanding the upset-forging of truncated conical sintered preforms, especially at higher die speeds.

REFERENCES

[1] Thomson, P. F. (1986). Densification of sintered metal compacts by cold deformation, Journal of Mechanical Working Technology, Elsevier, Vol. 13, No. 2, 219-227

[2] PM Parts Showcase, (2001). Cost savings win the day for PM parts, Metal Powder Report, Elsevier, Vol. 56, No. 7-8, 10-12, doi:10.1016/S0026-0657(01)80414-8

[3] Jha A. K.; Kumar S. (1994). Production of sinter-forged components, Journal of Materials Processing Technology, Elsevier, Vol. 41, No. 2, 143-169

[4] Singh S.; Jha A. K. (2001). Sintered preforms adds better value to aerospace components, Journal of Aerospace Engineering, Institution of Engineers (India), Vol. 82, 1-6

[5] Abdel-Rahman M.; El-Sheikh M. N. (1995). Workability in forging of powder metallurgy compacts, Journal of Materials Processing Technology, Elsevier, Vol. 54, No. 1-4, 97-102

[6] Sutradhar G.; Jha A. K. (1995). Cold forging of sintered polygonal discs, Journal of Production Engineering, Institution of Engineers (India), Vol. 76, 148-152

[7] Kim H.S.; Won C.W.; Chun B.S. (1998). Plastic deformation of porous metal with an initial inhomogeneous density distribution, Journal of Materials Processing Technology, Elsevier, Vol. 74, No. 1-3, 213–217

[8] Narayanasamy R.; Pandey K. S. (2000), A study on the barrelling of sintered iron preforms during hot upset forging, Journal of Materials Processing Technology, Elsevier, Vol. 100, No. 1-3, 87-94

[9] Chitkara N. R.; Liaghat G. H. (2001). Working pressure, deformation modes and fracture in open-piercing of cylindrical disks made of compacted sintered aluminium powder, International Journal of Advanced Manufacturing Technology, Springer, Vol. 17, 889-909

[10] Cho J. R.; Joo Y. S.; Jeong H. S. (2001), The Al-powder forging process: its finite element analysis, Journal of Materials Processing Technology, Elsevier, Vol. 111, No. 1-3, 204-209

[11] Singh S.; Jha A. K. (2001). Analysis of dynamic effects during high-speed forging of sintered preforms, Journal of Materials Processing Technology, Elsevier, Vol. 112, No. 1, 53-62

[12] Satsangi P. S.; Sharma P. C.; Prakash R. (2003), An elastic–plastic finite element method for the analysis of powder metal forging, Journal of Materials Processing Technology, Elsevier, Vol. 136, No. 1-3, 80-87

[13] Ohdar R. K.; Pasha S. (2003), Prediction of process parameters of metal powder preform forging using artificial neural network (ANN), Journal of Materials Processing Technology, Elsevier, Vol. 132, No. 1-3, 227-234
[14] Huang A.; Cheng J. (2004). An investigation into the forming limits of sintered porous materials under different operational conditions, Journal of Materials Processing Technology, Elsevier, Vol. 148, No. 3, 382-393
[15] Ranjan R. K.; Kumar S. (2004). High speed forging of solid powder discs of large slenderness ratio, Sadhana - Indian Academy of Sciences, Vol. 29, No. 5, 525–533
[16] Huang C. C.; Cheng J. H. (2004), An investigation into the forming limits of sintered porous materials under different operational conditions, Journal of Materials Processing Technology, Elsevier, Vol. 148, No. 3, 382-393
[17] Narayanasamy R.; Ramesh T.; Pandey K. S. (2005), Some aspects of workability studies in cold forging of pure aluminium powder metallurgy compacts, Materials Science and Technology, Ingenta, Vol. 21, No. 8, 912-917
[18] Singh S.; Jha A. K.; Kumar S. (2006). Analysis of rotary forging of sintered preforms, part-I: indentation phase, Tamkang Journal of Science and Engineering: An International Journal, Tamkang University Press, Vol. 9, No. 4, 313-324
[19] Singh S.; Jha A. K.; Kumar S. (2006). Analysis of rotary forging of sintered preforms, part-II: rotary phase, Tamkang Journal of Science and Engineering: An International Journal, Tamkang University Press, Vol. 9, No. 4, 325-330
[20] Yang T. S.; Hsu Y. C. (2006), Study on the bulging deformation of the porous metal in upsetting, Journal of Materials Processing Technology, Elsevier, Vol. 177, No. 1-3, 154-158
[21] Alves L. M. M.; Martins P. A. F.; Rodrigues J. M. C. (2006), A new yield function for porous materials, Journal of Materials Processing Technology, Elsevier, Vol. 179, 36-43
[22] Yang T.; Hsua Y. (2006). Study on the bulging deformation of the porous metal in upsetting, Journal of Materials Processing Technology, Elsevier, Vol. 177, No. 1-3, 154-158
[23] Singh S.; Jha A. K.; Kumar S. (2007). Dynamic effects during sinter forging of axi-symmetric hollow disc preforms, International Journal of Machine Tools & Manufacture, Elsevier, Vol. 47, 1101-1113
[24] Chandramouli R.; Pandey K. S.; Kandavel T. K.; Ashokkumar T.; Shanmugasundaram D. (2007). Influence of material flow constraints during cold forming on the deformation and densification behavior of hypoeutectoid P/M steel ring preforms, International Journal of Advanced Manufacturing Technology, Springer, Vol. 31, 926-932
[25] Pokorska I. (2007). Powder metallurgy materials in hot forming, Powder Metallurgy, Maney Publishing, Vol. 50, No. 4, 341-345
[26] Das P.; Sutradhar G.; Chakraborty T.; Patra S.; Mitra M. (2008). Cold forging of sintered hollow polygonal disks with barreling, Journal of Materials Processing Technology, Elsevier, Vol. 51, No. 1-4, 3188-3197.
[27] Pokorska I. (2008). Deformation of powder metallurgy materials in cold and hot forming, Journal of Materials Processing Technology, Elsevier, Vol. 196, No. 1-3, 15-32
[28] Jha A. K.; Kumar S. (1986). Deformation characteristics and fracture mechanisms during the forging of metal powder preforms, International Journal of Machine Tool Design and Research, Pergamon Press, Vol. 26, No. 4, 369-384
[29] Huang C.; Cheng J. (2002). Forging simulation of sintered powder compacts under various frictional conditions, International Journal of Mechanical Sciences, Elsevier, Vol. 44, No. 3, 489-507
[30] Rooks A. W. (1974). The effect of die temperature on metal flow and die wear during high-speed hot forging, Proceedings of the 15th International MTDR Conference, Birmingham, UK, 487
[31] Tabata T.; Masaki M. (1978). A Yield criterion for porous metals and analysis of axial compression of porous discs, Memories of Osaka Institute of Technology, Series-B, Science and Technology, Vol. 22, No. 2, 45
[32] Jha A. K.; Kumar S. (1994). Compatibility of sintered materials during cold forging", International Journal of Materials and Product Technology, Inderscience, Vol. 9, 281-299
[33] Avitzur B. (1968). Metal forming processes and analysis, McGraw Hill, New York, US
[34] Montgomery C. (1976). Design and analysis of experiments, John Wiley and Sons, New York, US
[35] Myers R. H. (1971). Response surface methodology, Allyn and Bacon, Boston, US. [17] Tan, G. J. (2000). The structure method and application of background value in grey system GM(1,1) Model (I), Systems Engineering - Theory & Practice, 20 (4), 98–103